Bioorganic & Medicinal Chemistry Letters 22 (2012) 4111–4116

Contents lists available at SciVerse ScienceDirect

Bioorganic & Medicinal Chemistry Letters

journal homepage: www.elsevier.com/locate/bmcl

Structure–activity relationship of a series of non peptidic RGD integrin antagonists targeting $\alpha_5\beta_1$: Part 1

Bénédicte Delouvrié [a,*], Katherine Al-Kadhimi [b], Jean-Claude Arnould [a], Simon T. Barry [b], Darren A.E. Cross [b], Myriam Didelot [a], Paul R. Gavine [c], Hervé Germain [a], Craig S. Harris [a], Adina M. Hughes [b], David A. Jude [b], Jane Kendrew [b], Christine Lambert-van der Brempt [a], Jean-Jacques Lohmann [a], Morgan Ménard [a], Andrew A. Mortlock [b], Martin Pass [b], Claire Rooney [b], Michel Vautier [a], Jennifer L. Vincent [b], Nicolas Warin [a]

[a] AstraZeneca, Centre de Recherches, Z.I. La Pompelle, B.P. 1050, Chemin de Vrilly, 51689 Reims, Cedex 2, France
[b] AstraZeneca Pharmaceuticals, Alderley Park, Macclesfield, Cheshire SK10 4TG, United Kingdom
[c] AstraZeneca R&D, Innovation Center China, Shanghai 201203, China

ARTICLE INFO

Article history:
Available online 21 April 2012

Keywords:
Integrin $\alpha_5\beta_1$ antagonist
Zwitterion
RGD integrin
Angiogenesis

ABSTRACT

Potent antagonists of the integrin $\alpha_5\beta_1$, which are RGD mimetics built from tyrosine are described. This letter describes the optimization of in vitro potency obtained by variation of two parts of the molecule, the basic group and the linker between the basic group and the phenyl central core.

The fibronectin receptor $\alpha_5\beta_1$ is a member of the integrin superfamily of heterodimeric glycoprotein receptors, which mediate cell-cell and cell-extracellular matrix interactions. $\alpha_5\beta_1$ is known to play a key role in the early stage of angiogenesis and is overexpressed in human tumor vasculature (e.g., colon and breast carcinomas).[1,2] Its overexpression has been associated with poor prognosis.[3] It was also demonstrated in animal models that inhibition of $\alpha_5\beta_1$ significantly reduced tumor angiogenesis and tumor growth.[4,5] Moreover, the combination of a VEGFR antibody with an $\alpha_5\beta_1$ antibody proved more beneficial than each agent alone to control tumor growth in several animal models, opening a new avenue for a best use of $\alpha_5\beta_1$ inhibitors in cancer.[6]

$\alpha_5\beta_1$ is a RGD integrin (like $\alpha_v\beta_{3,5,6}$ and $\alpha_{IIb}\beta_3$), in reference to the key recurrent arginine-glycine-aspartic acid (RGD) motif on the natural peptidic ligand fibronectin. The very few non peptidic small molecules reported to inhibit $\alpha_5\beta_1$ all mimic elements of this RGD peptidic sequence. Original spiro compounds of MW > 600 g/mol from Dupont were followed first by a series of trisubstituted pyrrolidines from Jerini, then more recently by a series of lower MW.[7–9] One compound of undisclosed structure, JSM6427, has recently completed a phase I study for age-related macular degeneration (AMD) with an intravitreal injection formulation.[5] The most advanced $\alpha_5\beta_1$ antagonists in clinic are the chimeric antibody Volociximab (PDL/Biogen),[4,10] and the small peptide ATN-161 (Attenuon),[11] currently in phase II trials. Here we describe the SAR of a series of non peptidic $\alpha_5\beta_1$ antagonists.

Minimal structural information has been reported on $\alpha_5\beta_1$ receptor itself but a crystal structure of the extracellular domain of $\alpha_v\beta_3$ in complex with a cyclopeptide inhibitor is available.[12] In the RGD integrins, the ligand binding is mediated through the RGD recognition motif which makes two key and conserved interactions with both α and β subunits. The carboxylate group of the aspartic acid coordinates with the metal-ion dependent adhesion site (MIDAS) located in the β subunit (herein referred to as the right hand side of the receptor), while the guanidine function of arginine is engaged in a bidentate salt bridge with a highly conserved aspartic acid residue in the α subunit (left hand side). The crystal structure of the cyclopeptide ligand bound to $\alpha_v\beta_3$ reveals that the distance between the basic and acidic moiety is about 13 Å. The strong sequence similarity between $\alpha_5\beta_1$ and $\alpha_v\beta_3$ around the RGD binding site allowed us to build a useful homology model of $\alpha_5\beta_1$ to support our design rationale.[13] The 2 key ionic interactions oriented us to develop zwitterionic molecules represented by the general structure in Figure 1.

The central core was initially fixed as a phenyl ring, starting materials being accessible as derivatives of tyrosine. Literature on $\alpha_4\beta_1$ integrin suggested to use the 2,6-dichlorophenylamide group as a suitable right hand part of the molecule.[14] Other groups also described the importance of 2,6-disubstitution pattern for $\alpha_5\beta_1$ selectivity.[9] Indeed, the 2,6-disubstitution twists the aromatic ring out of the plane of the amide bond and enables an ideal orientation

* Corresponding author.
E-mail address: benedicte.delouvrie@astrazeneca.com (B. Delouvrié).

0960-894X/$ - see front matter © 2012 Elsevier Ltd. All rights reserved.
http://dx.doi.org/10.1016/j.bmcl.2012.04.063

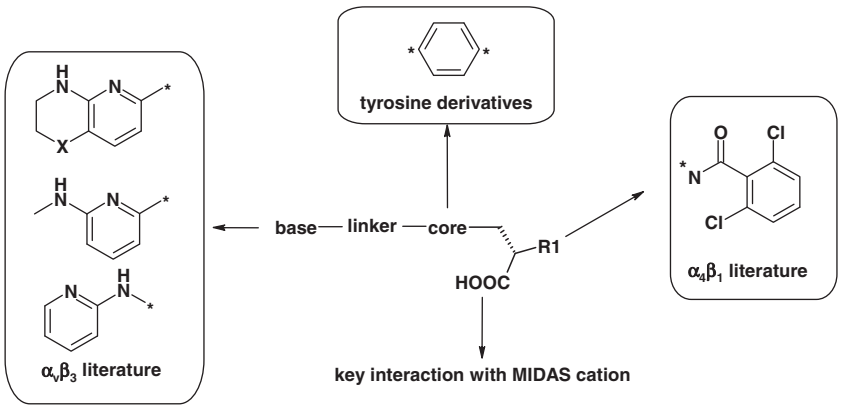

Figure 1. Rational design of $\alpha_5\beta_1$ inhibitors.

of the aromatic moiety inside the hydrophobic pocket of the β_1 subunit. Alternative literature exploring RGD mimics, especially those targeting $\alpha_v\beta_3$, described extensive optimization of the basic left hand part, suggesting that derivatives of 2-aminopyridines were suitable replacements of the fibronectin's arginine.[15] Having those fragments of the molecules set up, the nature and length of the linker needed to be optimized, driven by the homology model. This letter describes the SAR observed when varying the linker and the basic group of these new $\alpha_5\beta_1$ inhibitors.

The synthesis of compounds **1–22** was described previously and is summarized on Scheme 1.[16] The linker was introduced by a coupling reaction: Mitsunobu for X = O, Y = CH_2, Heck coupling for XY = HCCH, Sonogashira coupling for XY = CC and peptide coupling for X/Y = N, Y/X = C(O). These coupling reactions led to the methyl esters of general formula **23**. When required, a deprotection step of the basic nitrogen (most typically protected as a BOC) and/or a reduction step of unsaturated bonds could precede a saponification of **23** to afford the final carboxylic acids **1–22**.

Compounds were routinely evaluated using a binding assay and an adhesion assay in K562 cells.[16] For clarity of discussion, only a limited set of data on representative compounds is used to describe the SAR. When trends are exemplified by a single pair of compounds, it is to be understood that more examples exist to support the SAR described.

Linker variation: A preliminary docking study of compounds **1–3** in our $\alpha_5\beta_1$ homology model suggested that the ideal distance between the aminopyridine group and the carboxylic acid group to catch the two interactions with Asp227 and MIDAS would be obtained with the five atom linker compound **2** (Fig. 2). Indeed, both enzyme and cell IC_{50}s confirmed this hypothesis, **2** being significantly more potent than the shorter and longer linkers, respectively **1** and **3** (Table 1). Analogs of compounds **1–3** were made with a methylene linker and an alkyne linker, the best potency being obtained with the five atom linkers **4** and **5**.

The O-linker proved more potent than the methylene linker, as illustrated by the pairs **2–5**, **6–7**, **9–10**. This trend was observed on 18 matched pairs during our research program, as highlighted in Figure 3, with up to 20-fold better cell adhesion potency for the O-linked compounds. Although it is tempting to put forward the reduced conformational freedom of the O-linker, resulting in a decreased entropic penalty compared to the methylene linker to adopt the binding conformation, we cannot discount that the receptor would better accommodate a more hydrophilic O atom in this particular position.

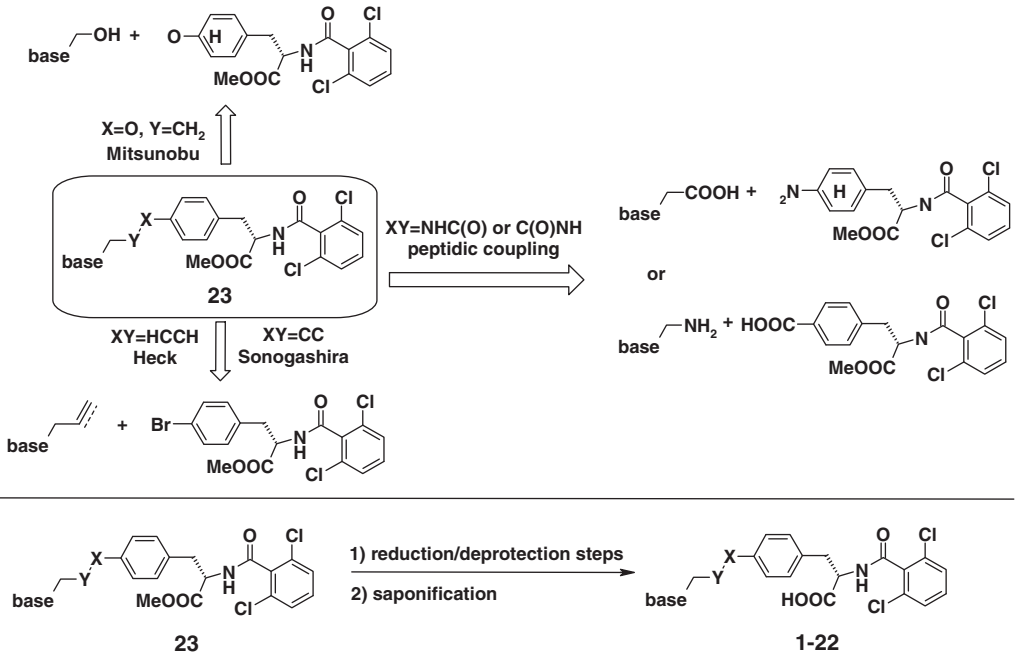

Scheme 1. General synthesis.

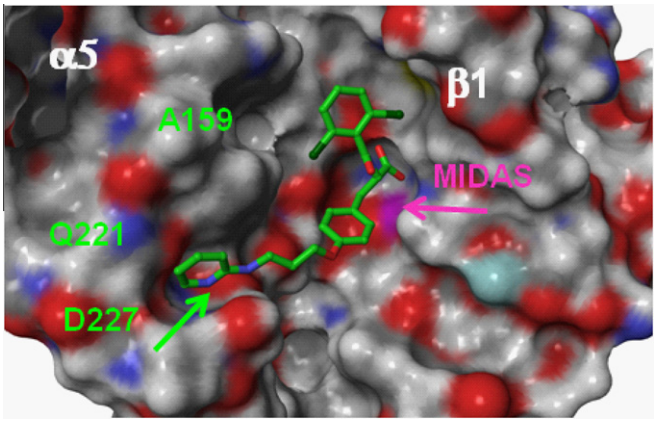

Figure 2. Compound **2** docked in $\alpha_5\beta_1$ homology model revealing the expected electrostatic interactions between the carboxylate group and the MIDAS site (β_1 unit) and between the bidentate salt bridge and Asp227 (α_5 unit).

The O- and CH_2-linkers were always significantly more potent than the alkyne linker analog (**4** vs **2** and **5**), possibly suggesting that a partially rigidified linker was not able to position the basic group to interact optimally with Asp227 when the flexible linear linkers could. However, not all flexible linear linkers were equally potent. Indeed, compound **6** (O-linker) was much more potent than compound **8** (CH_2O linker) and the O- and CH_2-linkers were more potent than the amide linkers (**11–12** vs **9–10**). This illustrated that in addition to the conformational and flexibility requirements, the electronic nature of the linker needs to be subtly adjusted to fit well with the surrounding amino acids residues of the integrin. Similar observations were reported with $\alpha_v\beta_3$ inhibitors.[17]

Basic group variation: The 6-methylamino-pyridin-2-yl (MAP) compounds **6–7** and the 5,6,7,8-tetrahydro[1,8]naphthyridin-2-yl (THN) compounds **9–10** were much more potent (up to >100-fold) than their 2-aminopyridinyl analogs **2** and **5** (Table 1). The small differences of pK_a (measured pK_as were spread only on ~1 unit in Table 1) might not explain the significant differences of potency. The salt bridge interaction with Asp227 seems stronger when the non aromatic N atom is positioned towards the end of the α_5 pocket rather than inserted into the linker chain.

In addition to aminopyridine derivatives (**2**, **6** and **9**), we also investigated other basic groups (Table 2). A basic aminoheterocycle appeared to be a pre-requisite for getting strong affinity for the receptor. This was reported on related $\alpha_5\beta_1$ inhibitors.[9] Aminobenzimidazole with the appropriate linker also gave an interesting level of potency as shown with compound **13**. The aminobenzimidazole proved more potent than the non basic aminobenzothiazole analog (**13** vs **14**). The pKa influence could also explain the decreased potency between the aminopyridine **2** and the non basic urea **15**. This could however be specific to α_5 since potent urea inhibitors of $\alpha_v\beta_3$ were reported.[18] We also noticed that a variety of monodentate basic groups were poor inhibitors of $\alpha_5\beta_1$, as examplified by the azetidine **16**. This is clearly different from the αIIbβ3 inhibitors, where for instance piperidines have reached high levels of in vitro potency.[19]

Figure 4 offers a possible explanation for these results. Comparison of the X-ray crystal structures of $\alpha_v\beta_3$, α_{IIb} β_3, and our 3D model of $\alpha_5\beta_1$ revealed subtle differences in the location of the conserved Asp in the β propeller groove of the respective α subunits.[12,20] In α_v, the conserved Asp218 is located on the side, at the entry of a shallow groove. Another Asp150 is present on the opposite side of this pocket, offering an extra H-bond interaction opportunity. Both Asp residues can indeed interact with the arginine, providing a particularly strong interaction. The bottom

Table 1
Linker optimization on compounds **1–12**

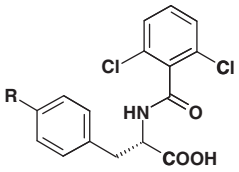

Compound	R	Binding IC_{50}, μM[a]	K562 cell adhesion IC_{50}, μM[a]	Measured basic pKa
1	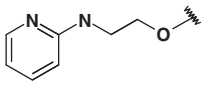	0.082	2.5	6.7
2	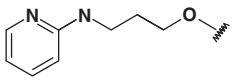	0.011	0.12	7.1
3	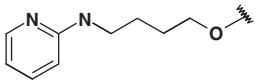	0.054	0.71	
4	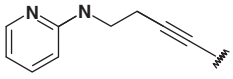	0.069	2.1	6.7
5	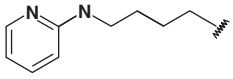	0.024	1.1	7.2
6	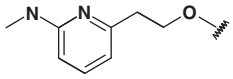	<0.001	0.007	7.0
7	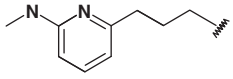	0.008	0.046	7.6
8	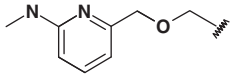	0.22	1.4[b]	6.4
9	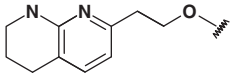	<0.001	<0.003	7.6
10	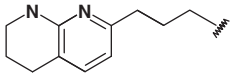	<0.001	<0.008	
11	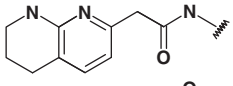	0.003	0.084	
12	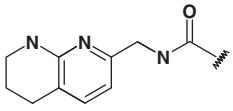	0.005	0.12	6.8

[a] Unless stated otherwise, numbers are a geometric mean of 2 or more values.
[b] $n = 1$ value.

of the groove is occupied by a Thr212. In α_5, Asp227 occupies the same location at the entry of the pocket than Asp218 in α_v, but the other (α_v)Asp150 is replaced by a small non polar Ala159 and (α_v)Thr212 in the bottom is changed for a larger Gln221.This decreases the negatively charged surface of the α_5 groove and slightly shortens it. The potential of (α_5)Gln221 to provide extra H-bond remains unclear. In α_{IIb}, the conserved Asp224 lies at the bottom of the groove, conferring a deeper character to this pocket. This affords both monodentate aliphatic and bidentate basic groups to bind, provided the monodentate base presents the N–H bond in the appropriate direction. Another consequence is that the optimal distance between the basic and acidic moieties is longer in $\alpha_{IIb}\beta_3$ than in $\alpha_v\beta_3$ or $\alpha_5\beta_1$ (~16 Å vs ~13 Å).

The piperazinopyridine **17** and the morpholinopyridine **18** were well tolerated, although less potent than the THN analog **9**, probably due to their lower pKa. Derivatives of the *N*-Methyl aminopyr-

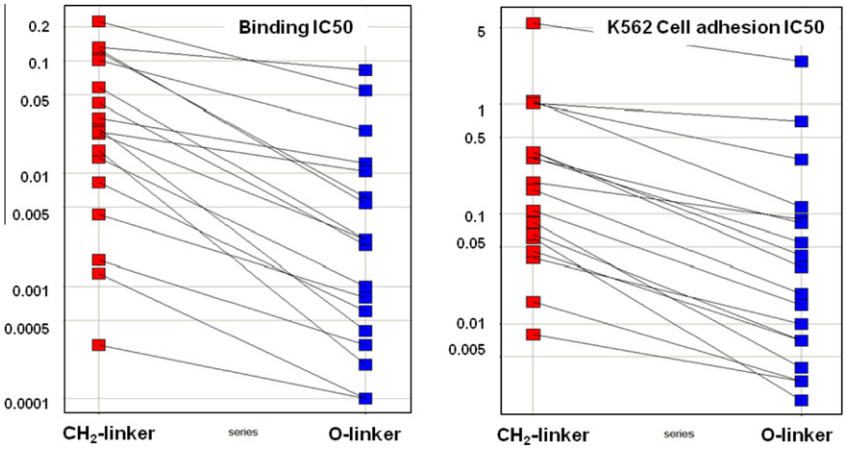

Figure 3. Binding and K562 cell adhesion IC_{50}s for all C- versus O-linker matched pairs.

Table 2
Basic group variation on compounds **2**,**6**,**9** and **13**–**22**

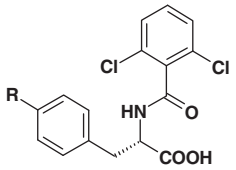

Compound	R	Binding IC_{50}, μM[a]	K562 cell adhesion IC_{50}, μM[a]	Measured basic pKa
2	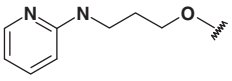	0.011	0.12	7.1
6	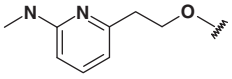	<0.001	0.007	7.0
9	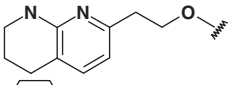	<0.001	<0.003	7.6
13	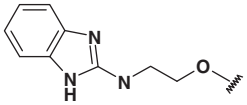	0.008	0.16	7.2
14	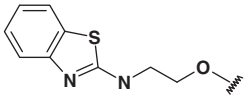	0.97	2.4[b]	4.3
15	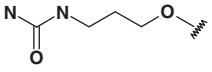	0.15	10	–
16	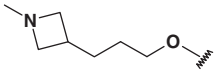	0.36[b]	58[b]	
17	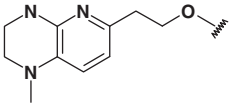	0.001	<0.008	7.1
18	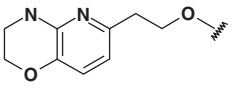	0.001	0.010	6.0
19	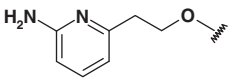	<0.001	0.009	

Table 2 (*continued*)

Compound	R	Binding IC_{50}, μM[a]	K562 cell adhesion IC_{50}, μM[a]	Measured basic pKa
20	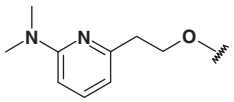	0.14	2.7[b]	
21	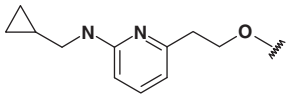	0.003	<0.041	
22	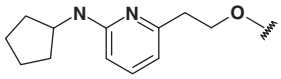	0.083	0.32[b]	6.8

[a] Unless stated otherwise, numbers are a geometric mean of 2 or more values.
[b] $n = 1$ value.

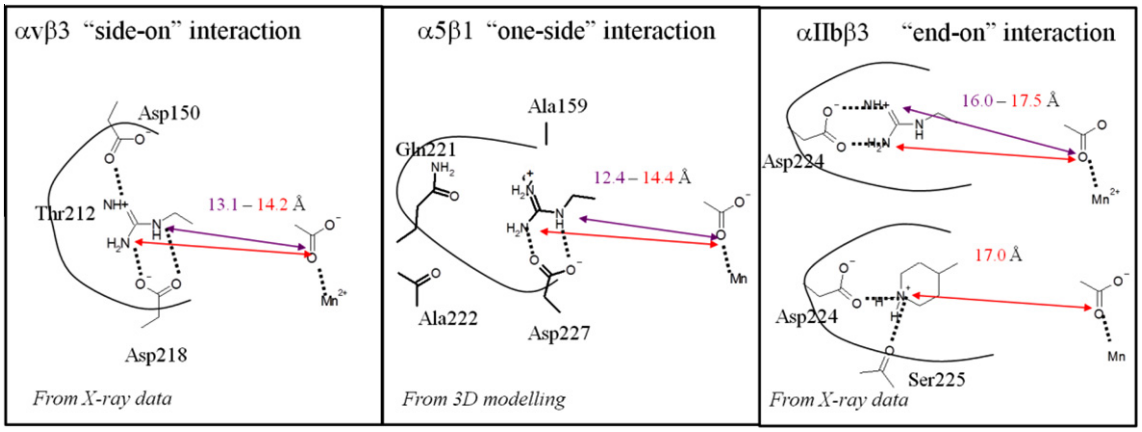

Figure 4. Interactions in the α_v, α_5 and α_{IIb} subunits.

Table 3
Cell adhesion assays +/− human serum albumin

Compound	% free in rat	Binding IC_{50}, μM[a]	K562 cell adhesion assay no HSA IC_{50}, μM[a]	K562 cell adhesion assay 630 μM HSA IC_{50}, μM[a]
9	0.7%	<0.001	<0.003	0.029
10	0.6%	<0.001	<0.008	0.45
17	1.5%	0.001	<0.008	<0.056

[a] All numbers are a geometric mean of 2 or more values.

idine **6** were made to explore the steric and electronic scope on the α_5 subunit. The des-methylated compound **19** was almost as potent as **6**. On the contrary, the *N,N*-dimethyl analog **20** showed a significant decrease of potency. This could either be due to a steric clash, or reflect the importance of a NH for a good binding to Asp227. Some steric hindrance could be tolerated, as examplified by compound **21**, but to a certain limit as shown by the potency decrease of cyclopentyl **22**. This is in agreement with the presence of the bulky Gln221 at the bottom of the groove.

During the course of the project, it appeared that our most potent compounds were reaching the lower limit of the cell adhesion assay run without human serum albumin (HSA). To better discriminate between potent compounds, we developed the same assay with HSA (630 μM concentration). Since typical binding to albumin across species was ~99% in this zwitterionic series, clear differences were seen between the cell assays with and without serum, as shown in Table 3. Compounds **9**, **10** and **17** were difficult to rank in the no serum assay, but **9** and **17** clearly appeared more potent than **10** in the full serum assay.

When targeting a specific RGD integrin, one has to evaluate selectivity versus other RGD integrins. It quickly appeared that these compounds were inactive against $\alpha_{IIb}\beta_3$ (IC50 >10 μM, data not shown). This can be explained by the distance difference highlighted on Figure 4. To assess the selectivity of our compounds against $\alpha_v\beta_3$, we developed cell adhesion assays that could differentiate selective from dual inhibitors.[21] The A375 cell adhesion assay with fibrinogen reflects binding mediated solely through $\alpha_v\beta_3$. Our series showed some inhibition in this assay (Table 4). It should however be noted that the level of potency was at least 10 fold lower than the Merck MK-0429 $\alpha_v\beta_3$ inhibitor.[22] The A375 cell adhesion assay with fibronectin reflects binding mediated by both α_5 and α_v integrins. The activity of our series for both $\alpha_5\beta_1$ and $\alpha_v\beta_3$ was confirmed using the A375 cell adhesion assay in presence of fibronectin without and with an $\alpha_v\beta_3$ inhibitor. Results showed modest ratios for our series (1.6–5.9) suggesting dual $\alpha_5\beta_1/\alpha_v\beta_3$ inhibition. In comparison, Jerini's compound was less potent against $\alpha_5\beta_1$ (K562 IC_{50} of 0.586 μM) but more selective for $\alpha_5\beta_1$ versus $\alpha_v\beta_3$ (ratio of 15).

Table 4
RGD integrin selectivity data[a]

Compound	A375 cell adhesion fibrinogen IC_{50}, μM[b]	A375 cell adhesion fibronectin IC_{50}, μM[b] without/with $\alpha_v\beta_3$ inhibitor (ratio)[c]
2	0.084	2.5/0.61 (4.0)
6	0.007	0.23/0.097 (2.4)
9	0.001	0.009/0.002 (4.5)
11	0.049	0.86/0.21 (4.0)
12	0.35	8.4/1.4 (5.9)
17	0.023	0.25/0.15 (1.6)
18	0.017	0.27/0.13 (2.1)
Jerini 1st series[d,e]	1.2	3.2/0.20 (15)
MK-0429[e]	0.0003	0.81/2.2 (0.4)

[a] All numbers are a geometric mean of 2 or more values.
[b] Assay performed in presence of Mg^{2+}.
[c] The Merck $\alpha_v\beta_3$ inhibitor MK-0429 was used at 1 μM concentration.
[d] 3-[2-[1-(Benzyloxycarbonyl)-5(*S*)-(pyridin-2-ylaminomethyl)pyrrolidin-3(*R*)-yloxy]acetamido]-N-(2,4,6-trimethylbenzoyl)-L-alanine.
[e] The Jerini and Merck compounds showed IC_{50}s in the K562 cell adhesion assay of 0.586 and 4.6 μM respectively.

In conclusion, we have developed potent inhibitors of $\alpha_5\beta_1$ which also carry activity against $\alpha_v\beta_3$. The homology model of $\alpha_5\beta_1$ and the structural data available on $\alpha_v\beta_3$ and $\alpha_{IIb}\beta_3$ have brought some rationale to the biological data while providing a better understanding on key elements of selectivity across the RGD integrins. SAR describing the influence of the core and the amide is described in the corresponding part 2 of this letter.

Acknowledgments

We would like to acknowledge the following scientists for their contribution in the synthesis or characterization of the compounds: Dominique Boucherot, Christian Delvare, Dr. Delphine Dorison Duval, Patrice Koza, Jacques Pelleter, Fabrice Renaud and Dr. Kin Tam.

References and notes

1. Yang, T. J.; Rayburn, H.; Hynes, R. O. *Development* **1993**, *119*, 123.
2. Kim, S.; Bell, K.; Mousa, S. A.; Varner, J. A. *Am. J. Pathol.* **2000**, *156*, 1345.
3. Adachi, M.; Taki, T.; Higashiyama, M.; Kohno, N.; Inufusa, H.; Miyake, M. *Clin. Cancer Res.* **2000**, *6*, 96.
4. Bhaskar, V.; Fox, M.; Breinberg, D.; Wong, M. H-L.; Wales, P. E.; Rhodes, S.; DuBridge, R. B.; Ramakrishnan, V. *Invest. New Drugs* **2008**, *26*, 7.
5. Umeda, N.; Kachi, S.; Akiyama, H.; Zahn, G.; Vossmeyer, D.; Stragies, R.; Campochiaro, P. A. *Mol. Pharmacol.* **2006**, *1820*, 69.
6. Chuntharapai, A.; Plowman, G.; Tessier-Lavigne, M.; Wu, Y.; Ye, W. WO2008/060645, 2008.
7. (i) Jadhav, P. K.; Smallheer, J. M. WO1997/033887, 1997.; (ii) Smallheer, J.; Weigelt, C. A.; Woerner, F. J.; Wells, J. S.; Daneker, W. F.; Mousa, S. A.; Wexler, R. R.; Jadhav, P. K. *Bioorg. Med. Chem. Lett.* **2004**, *14*, 383; (iii) Marinelli, L.; Meyer, A.; Heckmann, D.; Lavecchia, A.; Novellino, E.; Kessler, H. *J. Med. Chem.* **2005**, *48*, 4204.
8. Stragies, R.; Osterkamp, F.; Zischinsky, G.; Vossmeyer, D.; Kalkhof, H.; Reimer, U.; Zahn, G. *J. Med. Chem.* **2007**, *50*, 3786.
9. (i) Zischinsky, G.; Osterkamp, F.; Vossmeyer, D.; Zahn, G.; Scharn, D.; Zwintscher, A.; Stragies, R. *Bioorg. Med. Chem. Lett.* **2010**, *20*, 65; (ii) Zischinsky, G.; Osterkamp, F.; Vossmeyer, D.; Zahn, G.; Scharn, D.; Zwintscher, A.; Stragies, R. *Bioorg. Med. Chem. Lett.* **2010**, *20*, 380; (iii) Heckmann, D.; Meyer, A.; Marinelli, L.; Zahn, G.; Stragies, R.; Kessler, H. *Angew. Chem., Int. Ed.* **2007**, *46*, 3571; (iv) Heckmann, D.; Meyer, A.; Laufer, B.; Zahn, G.; Stragies, R.; Kessler, H. *ChemBioChem* **2008**, *9*, 1397.
10. (i) Tamaskar, I. *Drugs Future* **2010**, *35*, 16; (ii) Kuwada, S. K. *Curr. Opin. Mol. Ther.* **2007**, *9*, 92.
11. (i) Khalili, P.; Arakelian, A.; Chen, G.; Plunkett, M. L.; Beck, I.; Parry, G. C.; Donate, F.; Shaw, D. E.; Mazar, A. P.; Rabbani, S. A. *Mol. Cancer Ther.* **2006**, *5*, 2271; (ii) Cianfrocca, M. E.; Kimmel, K. A.; Gallo, J.; Cardoso, T.; Brown, M. M.; Hudes, G.; Lewis, N.; Weiner, L.; Lam, G. N.; Brown, S. C.; Shaw, D. E.; Mazar, A. P.; Cohen, R. B. *Br. J. Cancer* **2006**, *94*, 1621.
12. (i) Xiong, J. P.; Stehle, T.; Zhang, R.; Joachimiak, A.; Frech, M.; Goodman, S. L.; Arnaout, M. A. *Science* **2002**, *296*, 151; (ii) Gottschalk, K.-E.; Kessler, H. *Angew. Chem., Int. Ed.* **2002**, *41*, 3767; (iii) Tagaki, J.; Strokovich, K.; Springer, T. A.; Waltz, T. *Embo J.* **2003**, *22*, 4607. An $\alpha_5\beta_1$ homology model was described by Jerini in ref. 7iii.
13. Our $\alpha_5\beta_1$ homology model was built using the package Prime from Schrödinger (i) Jacobson, M. P.; Pincus, D. L.; Rapp, C. S.; Day, T. J. F.; Honig, B.; Shaw, D. E.; Friesner, R. A. *Proteins* **2004**, *55*, 351; (ii) Jacobson, M. P.; Friesner, R. A.; Xiang, Z.; Honig, B. *J. Mol. Biol.* **2002**, *320*, 597.
14. Davenport, R. J.; Munday, J. R. *Drug Discovery Today* **2007**, *12*, 569.
15. Cacciari, B.; Spalluto, G. *Curr. Med. Chem.* **2005**, *12*, 51.
16. Arnould, J.-C.; Delouvrié, B.; Ducray, R.; Lambert-Van Der Brempt, C. M. P. WO2007/141473, 2007.
17. Leonard, K.; Pan, W.; Anaclerio, B.; Gushue, J. M.; Guo, Z.; DesJarlais, R. L.; Chaikin, M. A.; Lattanze, J.; Crysler, C.; Manthey, C. L.; Tomczuk, B. E.; Marugan, J. J. *Bioorg. Med. Chem. Lett.* **2005**, *15*, 2679.
18. (i) Urbahns, K.; Harter, M.; Albers, M.; Schmidt, D.; Stelte-Ludwig, B.; Bruggemeier, U.; Vaupel, A.; Gerdes, C. *Bioorg. Med. Chem. Lett.* **2002**, *12*, 205; (ii) Urbahns, K.; Harter, M.; Vaupel, A.; Albers, M.; Schmidt, D.; Bruggemeier, U.; StelteLudwig, B.; Gerdes, C.; Tsujishita, H. *Bioorg. Med. Chem. Lett.* **2003**, *1071*, 13.
19. Scarborough, R. M.; Gretler, D. D. *J. Med. Chem.* **2000**, *43*, 3453.
20. (i) Xiao, T.; Takagi, J.; Coller, B. S.; Wang, J. H.; Springer, T. A. *Nature* **2004**, *432*, 59; (ii) Springer, T. A.; Zhu, J.; Xiao, T. J. *Cell Biol.* **2008**, *182*, 791.
21. To determine the ability of our compounds to inhibit $\alpha_v\beta_3$, a fibrinogen adhesion assay A375M cells was employed. A375M melanoma cells express a range of integrins including $\alpha_5\beta_1$, $\alpha_v\beta_3$ and $\alpha_v\beta_5$, however in the presence of the physiological cation Mg^{2+} binding to fibrinogen is mediated by $\alpha_v\beta_3$ integrin. This assay was validated with an α_v integrin blocking antibody (L230, active) and an $\alpha_5\beta_1$ integrin blocking antibody (M200, inactive).
A dual fibronectin adhesion assay was used to determine compound selectivity for $\alpha_5\beta_1$ over $\alpha_v\beta_3$. In the presence of Mg^{2+}, cell adhesion to fibronectin is mediated by both α_v and $\alpha_5\beta_1$ integrins. Inhibition of one integrin alone should not affect adhesion to fibronectin, as the other integrin can compensate. To eliminate adhesion via $\alpha_v\beta_3$ integrin, these assays were performed in the presence or absence of an $\alpha_v\beta_3$ inhibitor. The larger the shift in IC_{50} of cell adhesion to fibronectin from the absence to the presence of the $\alpha_v\beta_3$ inhibitor, the more $\alpha_5\beta_1$ selective the compound is.
22. The Merck compound MK-0429 demonstrated Proof of Concept in a phase II clinical trial against osteoporosis.